BJRS
BRAZILIAN JOURNAL OF RADIATION SCIENCES

doi.org/10.15392/2319-0612.2025.2708
2024, 12(4B) | 01-16 | e2708
Submitted: 2024-08-30
Accepted: 2025-07-15

Modeling nuclear fuel assemblies through porous zones in a Small Modular Reactor: fluid dinamic considerations

Gonçalves[a*], R. C.; Silva[b], G. C.; Schweizer[c], F. L. A.; Vinhas[c], P. A. M.; Carvalho[a], K. A.; Vieira[a], T. A. S.; Silva[a], V. V. A.; Barros[a], G. P.; Santos[a], A. A. C.

[a]Centro de Desenvolvimento da Tecnologia Nuclear
[b]Federal University of Minas Gerais
[c]Diretoria de Desenvolvimento Nuclear da Marinha

[*]Correspondence: cabralrebecag@gmail.com

Abstract: This work aims to qualify the use of porous zones for representing fuel assemblies of a proposed SMR reactor in numerical models to reduce the computational demand required to study these structures. It employs computational fluid dynamics (CFD) methods to calculate the conservation equations of mass, *momentum*, and energy within a control volume. Initially, a detailed fuel assembly geometry was created and used for isothermal simulations. The coefficients of porosity and pressure drop of the system were calculated based on the pressure drop and velocity results. These were then utilized to configure a second, simpler geometry of hexahedrons divided into thirteen sub-regions according to their cross-sectional area, each having different porosities and pressure drop coefficients. Finally, the results of the two simulations were compared to verify their convergence and allow the use of porous geometry. The outcomes suggest that, for models with a control volume significantly larger than a single fuel assembly, such as a complete nuclear reactor vessel, the use of porous zones is advantageous, as the variations in average velocity and pressure drop along the length of the structure are minor, with the maximum axial velocity variation of -10.99%. However, if the objective is to conduct a more detailed analysis of the entire assembly, this strategy is not recommended since some specific aspects of fluid behavior are not well captured, such as radial velocity differences.

Keywords: Porous Zones, Fuel Assembly, SMR, CFD.

BJRS
BRAZILIAN JOURNAL OF RADIATION SCIENCES

doi.org/10.15392/2319-0612.2025.2708
2024, 12(4B) | 01-16 | e2708
Submitted: 2024-08-30
Accepted: 2025-07-15

Modelagem de elementos combustíveis nucleares em um Reator Modular de Pequeno Porte: considerações fluidodinâmicas

Resumo: Este trabalho possui o objetivo de qualificar a utilização de zonas porosas para representação de elementos combustíveis de um reator SMR proposto em modelos numéricos, a fim de diminuir o custo computacional requerido para o estudo dessas estruturas. Para isso utiliza-se de métodos da fluidodinâmica computacional (CFD) para o cálculo das equações de conservação de massa, momentum e energia em relação ao volume de controle. Primeiramente, foi feita uma geometria detalhada do elemento combustível que foi utilizada para simulações isotérmicas. Os coeficientes de porosidade e de perda de carga do sistema foram determinados com base nos resultados de diferença de pressão e velocidade. Estes foram utilizados então para a configuração de uma segunda geometria, formada por hexaédros, composta por treze sub-regiões divididas de acordo com a área transversal de cada uma, sendo que cada uma possui porosidades e coeficientes de perda de carga diferentes. Por fim, os resultados das duas simulações foram comparados a fim de verificar sua convergência e para permitir a utilização da geometria porosa. Os resultados sugerem que, para modelos com um volume de controle significativamente maior que um elemento combustível, como um vaso de um reator nuclear completo, a utilização das zonas porosas é interessante, pois as variações da velocidade e diferença de pressão médias ao longo do comprimento da estrutura são pequenas, tendo o valor máximo de -10,99% na velocidade axial. Entretanto, caso o objetivo seja realizar uma análise mais detalhada de todo o conjunto, essa estratégia não é recomendada, pois certos aspectos específicos do comportamento do escoamento, como as diferenças de velocidade radial, não são bem representados.

Palavras-chave: Regiões Porosas, Elemento Combustível, SMR, CFD.

SBPR

1. INTRODUCTION

Small modular reactors (SMRs) are a class of reactors with a generation capacity of less than 300 MWe per unit and are named due to their particular geometric characteristics [1]. The term "small" refers to its reduced size compared to conventional reactors. At the same time, the word "modular" suggests that systems and components can be factory-assembled and transported as a unit to a location for installation. SMRs are a promising solution developed in response to the growing demand for clean, affordable, and reliable power generation in the current context of the world [2].

As a result of the reduced size of these reactors, their initial construction cost is expected to be lower [3]. Additionally, their modular characteristics enable operation under different conditions since more modules can be incorporated whether a higher power generation is desired. In terms of maintenance and surveillance purposes, modularity also plays a vital role in having available manufacturable and transportable equipment for replacement, unlike the current large power plants in which each plant has a unique design, and their parts are produced on demand and built on-site [3]. Finally, their design can be developed in a way that possibilitates the cogeneration of thermal energy and electrical power, which increases the overall efficiency of the nuclear power plant [4] and contributes to the decrease of global warming effects in the planet since this kind of energy production is considered a low carbon system [5].

To develop new designs for this class of reactors, a way to start is by studying a Pressurized Water Reactor (PWR), reducing the size of its components, and adding some other design characteristics, such as incorporating the steam generator inside the reactor vessel [6]. However, this type of geometry cannot be reduced in the same proportion for all reactor components, generating greater internal obstructions, thus modifying the thermo-

hydraulic and neutronic dynamics. Therefore, it is necessary to utilize an accurate and reliable tool to study the behavior of the small-scale system to develop new SMR projects. In this sense, the present paper proposes the utilization of Computational Fluid Dynamics - CFD to validate an SMR model scaled from a traditional PWR under the proposed methodology. CFD aims to predict fluid behavior in a system by numerically resolving its fundamental conservative equations of mass, *momentum,* and energy [7]. This tool has applications in different fields [8, 9, 10, 11] and wide validation from the scientific community, which justifies its utilization for this kind of study [12].

In this sense, Ansys CFX software was used to analyze the hydraulic behavior of a fuel assembly of an SMR [13]. Due to the geometry of these components and the need to obtain parameters with high precision in this region of the reactor, it was noted that the necessary mesh for the simulation requires a great refinement [14, 12]. Furthermore, these constraints imply the need for high computational power to simulate a complete reactor vessel utilizing these assemblies. Therefore, as a way to mitigate this problem, this work aims to qualify the application of porous zones, which correspond to regions of the domain that replace obstructed areas of the flow [15], with an equivalent pressure drop coefficient to adequately represent the fuel assemblies in the reactor core, considering that the simulation with the detailed geometry already is, to lower the computational cost of the numerical model.

2. MATERIALS AND METHODS

The first step towards the desired analysis is the mesh generation for the geometry in question. The assembly arrangement contains a typical 17 x 17 lattice with 260 fuel rods, one instrumentation tube, and 28 control/safety rods held by six spacer grids [16, 17, 18, 19, 20, 21]. However, generating the mesh for a complete fuel assembly is not reachable, given the available computational power in the Laboratório de Termo-Hidráulica e Neutrônica –

LTHN of Centro de Desenvolvimento da Tecnologia Nuclear - CDTN. Therefore, it was necessary to divide this domain into six regions, as shown in Figure 1a), along its length. The first one contains the inlet nozzle (IN) and the first spacer grid (SG); the next four consist of 1 spacer grid each, and the last one involves the last spacer grid and the outlet nozzle (ON). Moreover, it was decided to utilize the symmetry resource and create a geometry of only 1/8 of the fuel assembly, as shown in Figure 1b) lateral and superior view. This approach was necessary to decrease the computational power required even more.

Figure 1: a) Representation of the detailed geometry with the sub-region divisions and taps localisation. b) Representation of the simulated geometry with the sub-region divisions. c) Representation of the porous simulated geometry, with its different sub-regions.

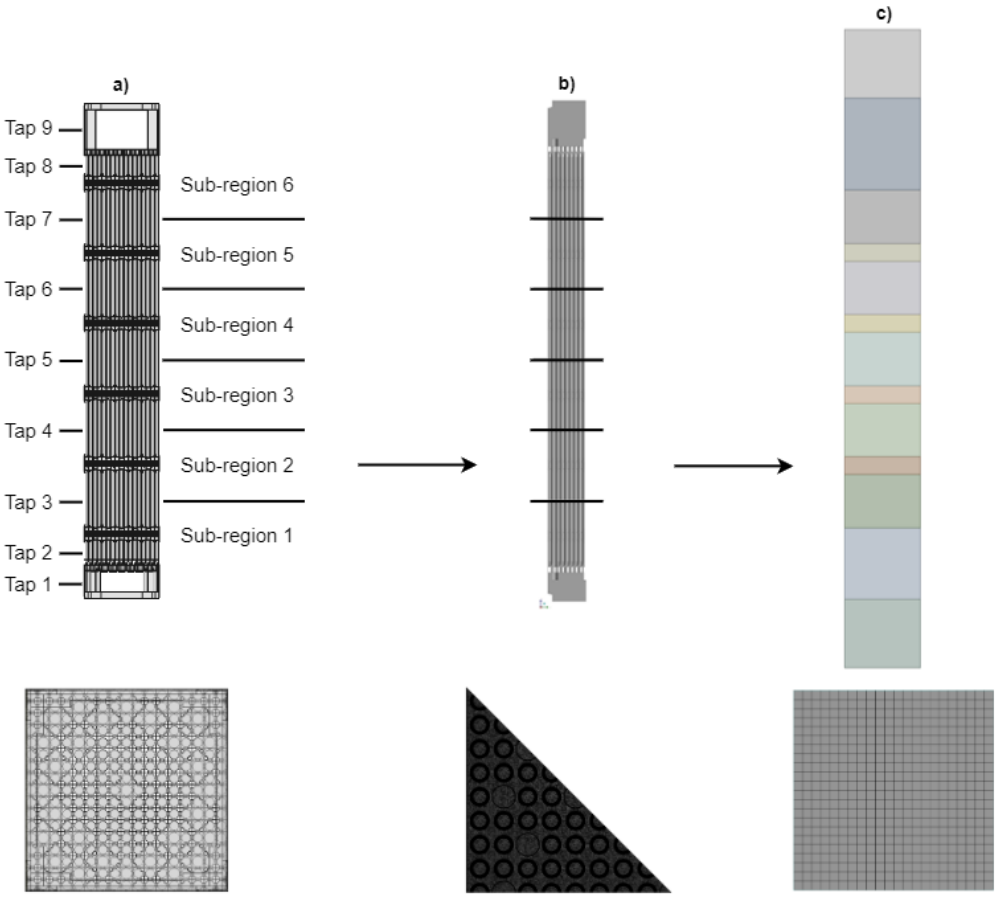

As a result, tetrahedral meshes were obtained for each sub-region of the detailed geometry, with a minimum of 68,512,605 elements/23,834,495 nodes (corresponding to zones between the 2nd and 5th spacer grids) and a maximum of 90,519,384

elements/26,605,441 nodes (corresponding to the region between the inlet nozzle and the 1st spacer grid). Simulations were then carried out involving each of these regions, where the outlet results of one simulation were utilized as inlet conditions for the following. Table 1 presents the boundary conditions and the simulation time from the calculations conducted for this article. The mesh refinement parameters and turbulence model used in the calculations were based on the group's previous verification and validation work [22, 23].

Table 1: Boundary conditions of the simulations.

Boundary Condition	Detailed Simulation (Each sub-region)	Porous Simulations
Mass Flow (Inlet)	21.32 kg/s [7]	21.32 kg/s [7]
Static Pressure (Outlet)	0 Pa	0 Pa
Temperature and Pressure	537.45 K and 131 bar	537.45 K and 131 bar
Mesh Averaged Element Size	5E-4 m	1E-2 m
Turbulence Model	k - ϵ	k - ϵ
Residual convergence criteria	1E-05	1E-06
Timestep	0.001	0.01
Max number of iterations	1500	500
Simulation Time	14h24	0h5

From the simulation of each region, it was possible to calculate the pressure drop (ΔP) for each zone under analysis. It is clear that, for regions with expansion or contraction factors for area, it is necessary to consider the dynamic pressure variation. This phenomenon is particularly notable in nozzle regions, where fluid velocity changes significantly before and after encountering the structure.

Therefore, with the velocity (v), pressure drop (ΔP), and density (ρ) values, it was possible to calculate the directional loss coefficients (K_{loss}) for each region using Equation (1) [24]. Then, dividing the result by the length of each domain, as specified in Ansys CFX

Manual [13], the parameters that would be inserted in the porous model configuration for Ansys CFX were obtained.

$$K_{loss} = \frac{2 \cdot \Delta P}{\rho \cdot v^2} \quad (1)$$

Furthermore, to configure the porous zones, the porosity volume is also used, which is the ratio of the fluid volume to the total physical volume. The free volume was calculated considering the nozzle, construction obstructions (such as screws), perforated plates, rod bundles, and spacer grids. This value mainly influences the resulting velocity of the region. The "true velocity formulation" or "full porous model" was used, for which porosity modifies all terms in the governing equations as well as the loss term [13].

It is important to note that, for the same fuel assembly, the coefficients vary according to the position on the z-axis since it varies according to the velocities observed in its length. Hence, to divide the different sub-regions of the porous geometry of the fuel assembly, the section area where the fluid flows was taken into account since it influences its resulting velocity. As a result, we obtained thirteen sub-regions, (Figure 1c), where the first and last are not porous, and the regions in between have similar velocities. For that, most regions include only one type of structure, spacer grids or rod bundles, except for the ones containing the nozzles, which contain rod bundles and one grid.

By replacing these parameters, new simulations were carried out using very simple meshes elaborated from a simpler geometry of hexahedrons, taking into account the porous coefficients. The whole geometry had 90,992 elements/106,329 nodes, 0.02% of the total number of elements necessary to represent the fuel assembly in a detailed manner, considering the six sub-regions. Subsequently, the total pressure and velocity values were extracted for each region of the fuel assembly to compare with the previous simulation.

It was essential to have similar results for velocity and pressure to ensure that the thermo-hydraulics of the porous model were trustworthy. For the fluid dynamics, both properties are

important. Still, velocity is important to the thermal analysis that is expected to be done afterward since it considers the kinetic energy of the fluid to calculate the energy flux [13].

Moreover, the extended uncertainty of the models utilized for this study was also calculated [25, 12]. This magnitude takes into account all the components of uncertainty that can be present in a simulation and follows Equation (2). In this Equation, U_d represents the uncertainty associated with the discretization process and can be calculated through the V&V20 norm [26], resulting in the most significant component of the uncertainty. U_{ite} is related to the simulation residuals, in these cases lower than $1E10^{-4}$. U_a is associated with the rounding of the results during the calculations, and since it was used double precision, this value is fixed in $1E10^{-16}$. This result creates a range where the solution of the calculus lies, with a confidence interval of 95%, and it is presented for both simulations in Figure 4, displayed in Section 3.

$$U_{ext} = \sqrt{U_d^2 + U_{ite}^2 + U_a^2} \tag{2}$$

3. RESULTS AND DISCUSSIONS

Figure 2 presents the side view of the complete detailed assembly with the results for the velocity vector, where the six simulations performed to complete the entire assembly can be observed. This simulation shows a significant jet behavior after the inlet nozzle and even after the second spacer grid, highlighting how much the structure's obstructions influence the flow.

Figure 2: Velocity field of the simulations with the detailed geometry of the fuel assembly.

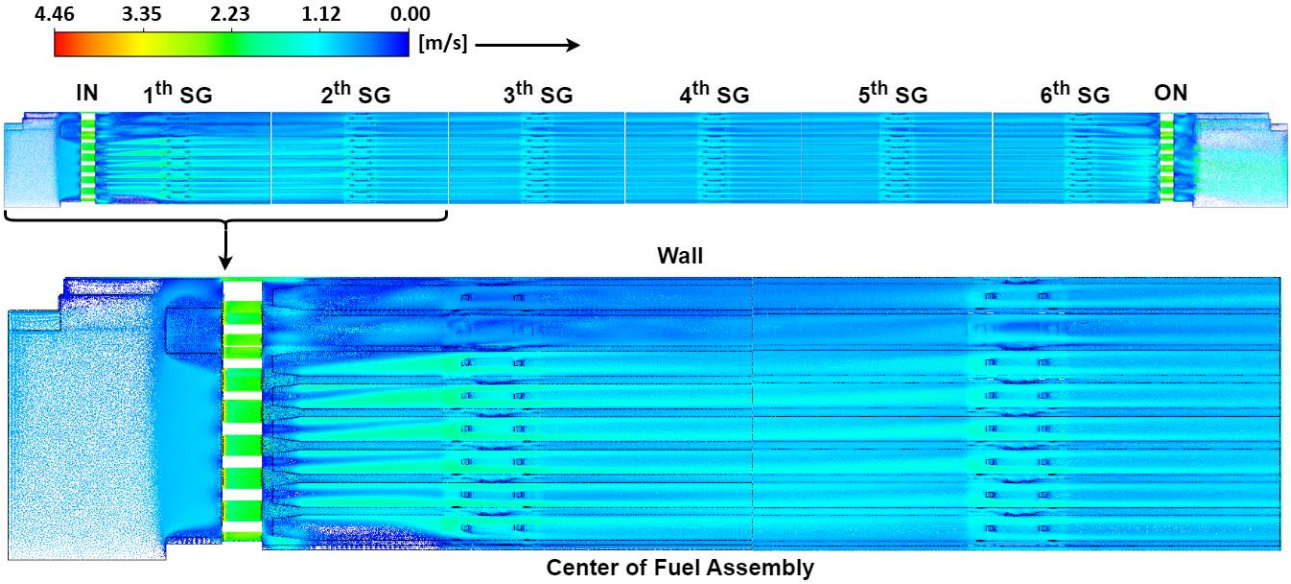

Another interesting view is the comparison that can be made between the velocities in the planes of the pressure taps presented in Figure 3. By observing the planes, it can be noticed how the flow became more homogeneous along the fuel assembly. In the initial planes, the highest velocity was concentrated in the central subchannels of the assembly, near the origin of the graph, which can also be observed in Figure 2. This occurred due to the large obstructions of the nozzle, which are mainly located at its extremities. In the final planes, from the 4th grid (plane 6) onwards, the velocity difference is already less significant along the subchannel.

Another important information that can be extracted from Figure 2 and Figure 3 is that it is possible to observe a decrease in the velocity in the subchannels near the instrumentation tubes. This outcome is relevant for a potential subsequent analysis to identify hot spots within the reactor core. In these areas, the velocity is lower, and the likelihood of encountering stagnant flow regions and energy accumulation is higher.

Figure 3: Velocity field of the nine taps from the simulations with the detailed geometry of the fuel assembly.

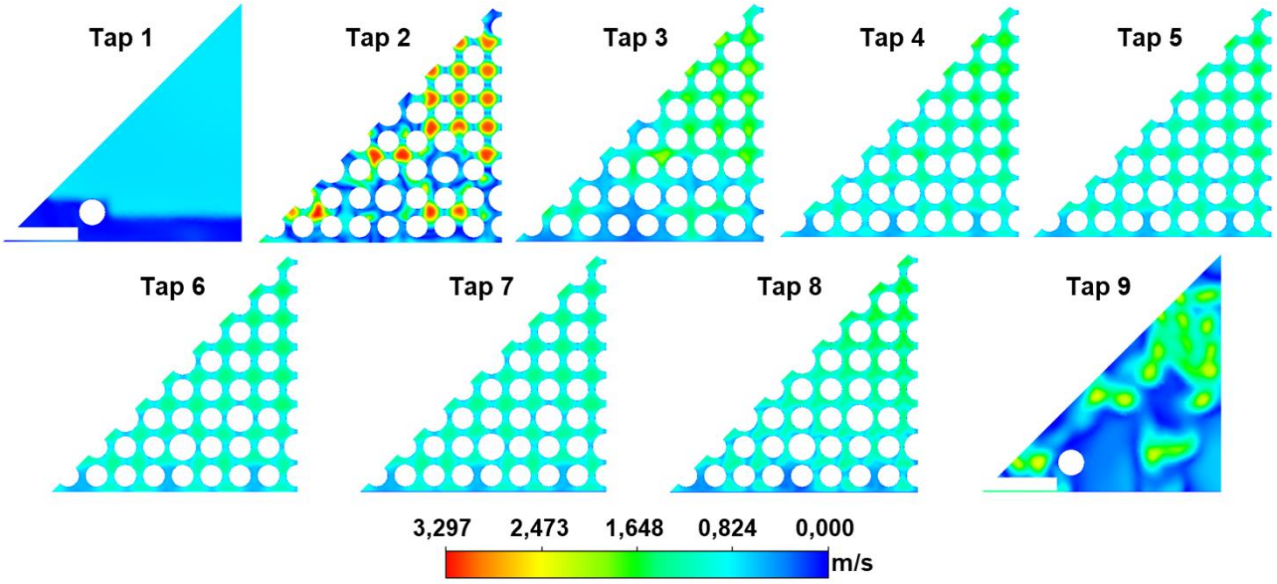

The comparison between the data obtained with the detailed simulation and the simulation with the porous domain allows the construction of the graphs shown in Figure 4. The length values were divided by the hydraulic diameter of the rod bundles region and the values of velocity and pressure were normalized using a reference value for each magnitude. In the areas of the nozzles, the error for the velocity is greater when compared to the other regions due to the considerable variation in the cross-sectional area, which generates different velocity values throughout the domain. Therefore, to use these data, it was necessary to use an average velocity value for the region, which is also plotted in the figure.

Figure 4: Comparative graphics of pressure and velocity between the detailed and porous simulation.

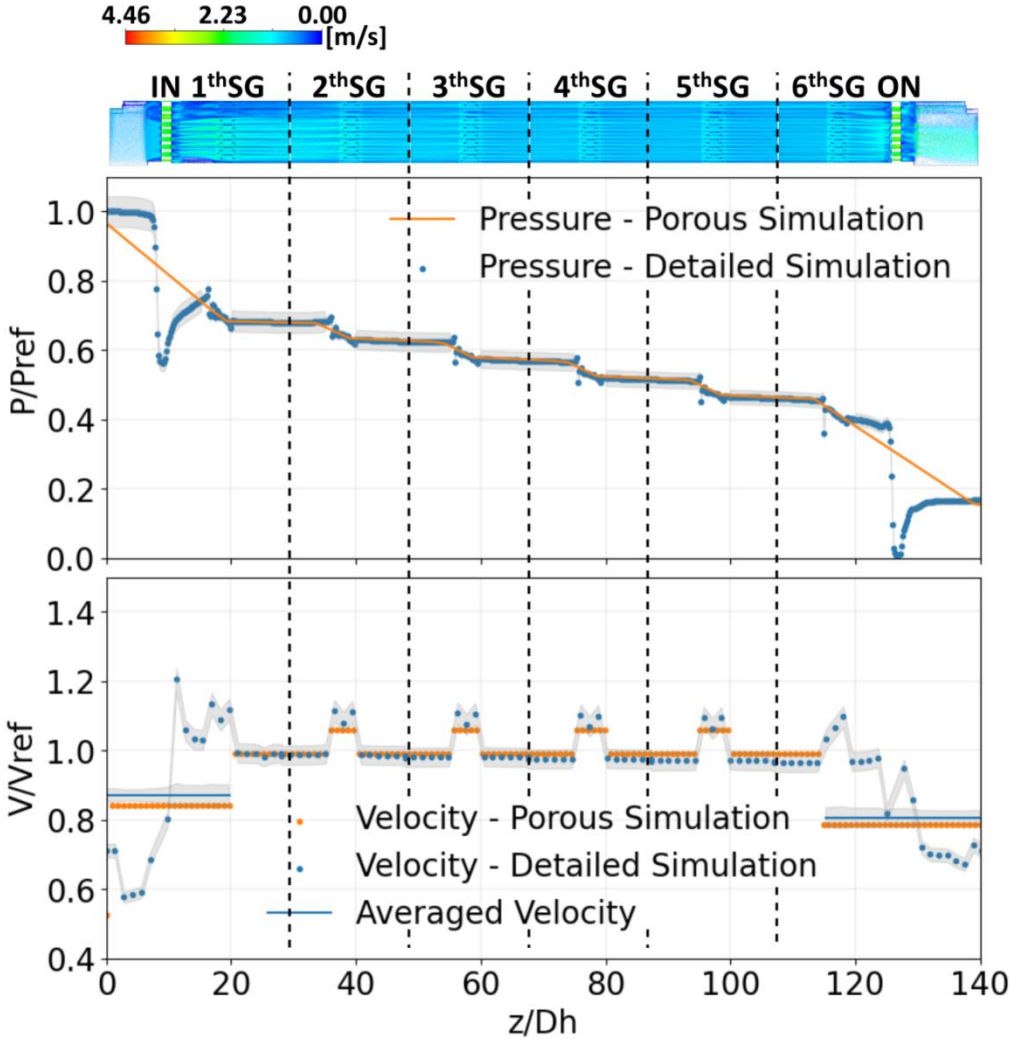

Table 2 provides the variations observed between the porous and detailed simulations for velocity and pressure drop. The values obtained for the velocities in the simulation are very close to each other, presenting a maximum value of approximately -10.99% for the axial direction. This value can be explained due to the various cross-section areas in the first and last sub-regions. The velocity of each region depends on the area value to maintain the mass balance, and since they do not have a fixed value in them, it was necessary to use an averaged value to calculate the coefficients, which can generate bigger values for the variations. The convergence of this parameter is essential to verify this methodology because, in a porous

domain, porosity is responsible for determining the velocity. Thus the proximity of the values presented in Figure 4 indicates that this model is valid for carrying out this type of simulation.

Table 2: Parameters utilized to configurare the porous sub-regions and the variation from the detailed geometry simulations.

Sub-region	Components	Porosity	K_{loss}	Variation (velocity)	Variation (ΔP)
1	Inlet nozzle and 1st spacer grid	0.63	14.66	-7.78%	0.00%
2	Rod bundle	0.53	0.15	-0.27%	0.02%
3	2nd spacer grid	0.50	1.10	-3.95%	0.00%
4	Rod bundle	0.53	0.29	0.17%	-0.01%
5	3rd spacer grid	0.50	1.13	-3.35%	0.00%
6	Rod bundle	0.53	0.30	0.72%	0.00%
7	4th spacer grid	0.50	1.12	-2.79%	0.00%
8	Rod bundle	0.53	0.28	1.25%	0.00%
9	5th spacer grid	0.50	1.12	-2.24%	0.00%
10	Rod bundle	0.53	0.30	1.77%	0.02%
11	6th spacer grid and outlet nozzle	0.67	15.03	-10.99%	0.00%

In relation to Total Pressure, influenced predominantly by the value of the pressure drop coefficient, it is clear that the values are even closer, presenting a maximum variation of approximately 0.02%. This indicates that the software correctly captures the reactor's hydraulic dynamic even when using porous regions.

4. CONCLUSIONS

When observing the proximity of values obtained in pressure and velocity, it is clear that using the porous models allows obtaining results consistent with the literature and the detailed model using lower computational power. It was shown in other work that the error margin in simulations regarding fuel assemblies should be lower than 20% for all measured properties. Since the most significant error found in this study is -10.99% for the axial

velocity in a specific height, we can conclude that the utilization of porous regions to substitute complex geometries in a domain would not influence the simulation in a way that is going to compromise the final results.

This way, it is possible, for example, to build a reactor's vessel model replacing the nucleus for the porous geometry, which is a methodology that facilitates the development of other SMR projects in centers with lower computational capability. Besides that, one disadvantage of this methodology is that it is not possible to capture local events in the domain, such as the ones that were presented in the results, such as the decrease of velocity near instrumentation tubes and closer to the walls and the water jet behavior near the nozzles.

In short, to determine whether using porous zones is appropriate for a model, it is essential to analyze the objective of the simulation. For a micro-level analysis, porous zones may not be beneficial, as certain localized events may be overlooked. However, porous zones can provide valuable insights for a macro-level analysis where the fuel assembly is considered a component within the entire control volume. Future work will aim to obtain results for both geometries used in the project, factoring in power distribution within the rod bundles and thermal exchange with the coolant. This will enable a more comprehensive analysis, taking into account the thermal-hydraulics of the fuel assembly.

ACKNOWLEDGMENT

The following Brazilian institutions support this work: Comissão Nacional de Energia Nuclear (CNEN); Fundação para o Desenvolvimento Tecnológico da Engenharia (FDTE); Fundação de Amparo à Pesquisa do Estado de Minas Gerais (FAPEMIG); Conselho Nacional de Desenvolvimento Científico e Tecnológico (CNPq), Coordenação de Aperfeiçoamento de Pessoal de Nível Superior (CAPES) and Financiadora de Estudos e Projetos (FINEP).

CONFLICT OF INTEREST

All authors declare that they have no conflicts of interest.

REFERENCES

[1] LIOU, Joanne. International Atomic Energy Agency. Disponível em: https://www.iaea.org/newscenter/news/what-are-small-modular-reactors-smrs. Acesso em: 19 jul. 2024.

[2] AMIN, Md Ruhul et al. A Review on the Future of SMR Reactors in Nuclear Energy. **Energy and Thermofluids Engineering**, v. 4, p. 17-23, 2024.

[3] HEDAYAT, Afshin. A review of advanced Small Modular Reactors (SMRs) through a developed PIRT methodology. **Radiation Physics and Engineering**, 2023.

[4] KANG, Seong Woo; YIM, Man-Sung. Coupled system model analysis for a small modular reactor cogeneration (combined heat and power) application. **Energy**, v. 262, p. 125481, 2023.

[5] MATHEW, M. D. Nuclear energy: A pathway towards mitigation of global warming. **Progress in Nuclear Energy**, v. 143, p. 104080, 2022.

[6] FERNÁNDEZ-ARIAS, Pablo; VERGARA, Diego; ANTÓN-SANCHO, Álvaro. Bibliometric review and technical summary of PWR small modular reactors. **Energies**, v. 16, n. 13, p. 5168, 2023.

[7] Simscale. Disponível em: https://www.simscale.com/docs/simwiki/cfd-computational-fluid-dynamics/what-is-cfd-computational-fluid-dynamics/. Acesso em: 25 abr. 2023.

[8] WANG, Mingjun et al. A review of CFD studies on thermal hydraulic analysis of coolant flow through fuel rod bundles in nuclear reactor. **Progress in Nuclear Energy**, v. 171, p. 105175, 2024.

[9] WIJESOORIYA, Kasun et al. A technical review of computational fluid dynamics (CFD) applications on wind design of tall buildings and structures: Past, present and future. **Journal of Building Engineering**, v. 74, p. 106828, 2023.

[10] BASRI, Ernnie Illyani; BASRI, Adi Azriff; AHMAD, Kamarul Arifin. Computational fluid dynamics analysis in biomimetics applications: a review from aerospace engineering perspective. **Biomimetics**, v. 8, n. 3, p. 319, 2023.

[11] CHEKIFI, Tawfiq; BOUKRAA, Moustafa. CFD applications for sensible heat storage: A comprehensive review of numerical studies. **Journal of Energy Storage**, v. 68, p. 107893, 2023.

[12] SANTOS, A. A. C. Investigação numérica e experimental do escoamento de água em feixe de varetas representativo de elementos combustíveis nucleares de reatores do tipo PWR. 2012. **PhD Theses**. Universidade Federal de Minas Gerais, Belo Horizonte, 2012.

[13] Ansys INC. **Ansys CFX – Solver Theory Guide**. Canonsburg & United States, 2009.

[14] HAMMAN, Kurt D.; BERRY, Ray A. A CFD simulation process for fast reactor fuel assemblies. **Nuclear Engineering and Design**, v. 240, n. 9, p. 2304-2312, 2010.

[15] TUSAR, Mehedi Hasan et al. Porous media model simulates thermal-hydraulics of nuclear research reactors with flat and curved plate fuel assembly. **International Communications in Heat and Mass Transfer**, v. 153, p. 107334, 2024.

[16] VETTORAZZI, J. L. A importância do desenvolvimento do laboratório de geração nucleoelétrica (LABGENE) para a construção do submarino de propulsão nuclear. 2007. **PhD Theses**. Escola Superior de Guerra, Rio de Janeiro, 2012.

[17] SINIVAL, S. N. da. Indústria da Construção e Reparação Naval. Disponível em: http://sinaval.org.br/2020/06/labgene-nuclep-recebe-visita-de-autoridades-para-conhecerem-a-fabricacao-do-bloco-40-do-reator/. Acesso em: 12 jun. 2024.

[18] KIM, K.-T. The effect of fuel rod loading speed on spacer grid spring force**. Nuclear engineering and design**, Elsevier, v. 240, n. 10, p. 2884–2889, 2010.

[19] YOO, Y.; KIM, K.; EOM, K.; LEE, S. Finite element analysis of the mechanical behavior of a nuclear fuel assembly spacer grid. **Nuclear Engineering and Design**, Elsevier, v. 352, p. 110179, 2019

[20] KING, R. A. Nuclear fuel assembly bottom nozzle plate. **[S.l.]: Google Patents**, 1991. US Patent 5,009,839.

[21] HERNANDEZ-AVELLANEDA, A.; JIMENEZ, G.; REY, L.; MARTINEZ-MURILLO, J. C. Modelling fuel assembly flow nozzles in a spent nuclear fuel dry cask using cfd codes. **Annals of Nuclear Energy**, Elsevier, v. 181, p. 109540, 2023.

[22] SANTOS, Andre AC; BARROS FILHO, Jose Afonso; NAVARRO, Moyses A. Verification and validation of a numeric procedure for flow simulation of a 2x2 PWR rod bundle. **International Nuclear Atlantic Conference – INAC**, 2011.

[23] NAVARRO, Moysés A.; SANTOS, André AC. Evaluation of a numeric procedure for flow simulation of a 5× 5 PWR rod bundle with a mixing vane spacer. **Progress in Nuclear Energy**, v. 53, n. 8, p. 1190-1196, 2011.

[24] SCHWER, L. American Society of Mechanical Engineers. ASME V&V 20 - Standard for Verification and Validation in Computational Fluid Dynamics and Heat Transfer. New York, 2009.

[25] FOX, R. W.; MCDONALD, A. T.; PRITCHARD, P. J. **Introduction to Fluid Mechanics**. Hoboken, NJ, US: John Wiley & Sons, 1998. p. 235.

[26] CASTRO, H. F. P. Avaliação termo-hidráulica experimental de grades espaçadoras comerciais para reatores PWR e de protótipo fabricado por impressora 3D. 2020. **PhD Theses**. Universidade Federal de Minas Gerais, Belo Horizonte, 2020.

LICENSE